

Thermodynamics of DNA packaging inside a viral capsid: the role of DNA intrinsic thickness

Davide Marenduzzo¹ and Cristian Micheletti²

¹ Department of Physics, Oxford University, 1 Keble Road, Oxford OX1 3NP, United Kingdom

² International School for Advanced Studies (S.I.S.S.A.) and INFN, Via Beirut 2-4, 34014 Trieste, Italy

(Dated: October 5, 2018)

We characterize the equilibrium thermodynamics of a thick polymer confined in a spherical region of space. This is used to gain insight into the DNA packaging process. The experimental reference system for the present study is the recent characterization of the loading process of the genome inside the $\phi 29$ bacteriophage capsid. Our emphasis is on the modelling of double-stranded DNA as a flexible thick polymer (tube) instead of a beads-and-springs chain. By using finite-size scaling to extrapolate our results to genome lengths appropriate for $\phi 29$, we find that the thickness-induced force may account for up to half the one measured experimentally at high packing densities. An analogous agreement is found for the total work that has to be spent in the packaging process. Remarkably, such agreement can be obtained in the absence of any tunable parameters and is a mere consequence of the DNA thickness. Furthermore, we provide a quantitative estimate of how the persistence length of a polymer depends on its thickness. The expression accounts for the significant difference in the persistence lengths of single- and double-stranded DNA (again with the sole input of their respective sections and natural nucleotide/base-pair spacing).

I. INTRODUCTION

The goal of the present study is to characterize the equilibrium thermodynamics of a thick polymer chain confined in a spherical cavity. In particular we aim at establishing what force is necessary to apply, and how much energy is to be spent, to achieve a given packing density for the polymer. This problem is intimately related to the problem of DNA packaging inside a viral capsid^{1,2,3}, which is under an increasing theoretical and experimental attention^{4,5,6,7,8,9,10}. At variance with previous studies we model explicitly the double-stranded (ds) DNA as a cylindrical tube with a finite thickness (as opposed to a beads-and-springs model) and study how it impacts on the force and work required to package it. We shall further discuss how a finite thickness induces a non-negligible persistence length in a polymer. The experimental reference for the present study is provided by a series of experiments⁴ where the loading process of DNA inside the $\phi 29$ virus head was followed under controlled conditions. In this situation, the 6.6 μm long double-stranded DNA polymer was fed by a molecular motor inside the virus head, a prolate 54 nm by 42 nm icosahedron^{2,4,11}. By using suitable force-feedback measurements it has been possible to carefully measure the force exerted by the motor at various stages of the loading process, and hence the total energy required for the whole packaging process. It has been found⁴ that the internal force exerted by the packaged DNA against the $\phi 29$ capsid walls (which has to be overcome by the portal motor), displays a dramatic increase during the final loading stages. In particular, the maximum value attained by this internal force is ~ 50 pN. This is a strikingly large number when compared to typical forces encountered at the molecular and cellular scale.

In a recent study⁶, a molecular dynamics simulation has been used to characterize the dynamical packaging of DNA in a spherical cavity. In that approach, the double stranded DNA was coarse-grained in a beads-and-strings chain subject to self-interaction. Interestingly, it was found that, at high packing densities, the resistance to packaging was not dominated by the DNA self-interaction (whether attractive or repulsive). An insight into this result can be obtained by a soluble mean-field model, presented later, which highlights how the divergence of the packing force at high density is not controlled by self-interactions.

These results stimulate the search for an alternative physical mechanism responsible for the onset of the large packaging pressure encountered e.g. in $\phi 29$. For this reason, we adopted a minimal model where DNA is treated as a thick chain of equispaced beads. Since the DNA self-attraction or repulsion does not appear to be crucial at high packing densities, we have intentionally kept the model at the simplest level and thus avoided the introduction of any explicit treatment of the known self-interaction terms¹². The only two parameters entering in our model are the spacing between the beads and the chain thickness; we do not attempt any tuning of these parameters but, instead, adopt the corresponding values desumed from the experimental literature. In particular, the natural base spacing is set to 0.34 nm while the radius of hydrated double-stranded DNA is taken as 1.25 nm². Note that in this work the thickness of a tube is defined as the radius of its circular section taken normally with respect to the tube centerline.

As we shall show below, the appropriate treatment of the finite thickness of the biopolymer allows to account for a variety of elastic properties of DNA in a natural way, even in the absence of additional phenomenological parameters, such as the bending rigidity, that are used in standard DNA coarse-grained models. For example, it will be shown that the mere difference in thickness of single-stranded and double-stranded DNA can account for the large change in the respective persistence lengths. More importantly, by considering the force necessary to compactify thick chains of increasing number of beads, we estimate the packaging force (and work) which turns out to be in good quantitative agreement with experimental measures for $\phi 29$ under the same density conditions. The present analysis involves finite-size scaling techniques to extrapolate results obtained in

equilibrium stochastic simulations of chains with up to 200 beads. The most compact conformations obtained for such lengths reveal the clear tendency of thick polymers to occupy the spherical cavity by adopting a spool-like conformation, consistently with previous expectations^{2,7,10} and with the recent numerical study of Kindt *et al.* with a different model⁶.

II. THEORY AND METHODS

Due to the large number of atomic constituents of both inorganic and biological polymers, it is necessary to resort to suitably simplified models in order to characterize their physical behaviour by means of analytical or numerical studies. Customarily the polymeric chain is coarse-grained into a succession of discrete beads. Besides capturing the effect of chain connectivity through the introduction of suitable strings or springs between consecutive beads, it is usually necessary to introduce appropriate interactions between the beads in order to capture the salient physical features of the given system. For the case of ds DNA the latter would include effects such as strands self-interaction (either attractive or repulsive) and bending rigidity. As a useful term of comparison for the present and previous numerical studies of DNA packaging, it is useful to consider a mean-field model (inspired by the treatment in Refs.^{13,14}) which, while incorporating the above mentioned features, is still amenable to an analytic treatment. This model consists of a polymer chain of N beads embedded in a discrete three-dimensional space and subject to a contact interaction, ϵ , and a bending rigidity (corner penalty), h . Within a mean-field picture^{13,14} it is possible to obtain explicit expressions for the free energy, F_N and loading force, f , required to package the chain inside a cube of side L :

$$\frac{\beta F_N(x)}{N} = \frac{1-x}{x} \log(1-x) + \beta\epsilon(1-3x) - \log \left[\frac{2 + 4 \exp(-\beta h)}{e} \right], \quad (1)$$

$$a \beta f(x) = -\log(1-x) + \beta\epsilon(1-6x) - \log[2 + 4 \exp(-\beta h)] \quad (2)$$

where x is the density $x = N/L^3$, $\beta = (k_B T)^{-1}$ with k_B the Boltzmann constant and a is the unit length in the system. It is important to notice that the free-energy per bead, F_N/N depends on N and L only through the density x ; this fact will be exploited to analyze the results for our confined off-lattice chains with finite thickness.

Despite the simplified nature of the mean field model, the approximate force of expression (3) provides a useful starting point for both understanding recent packaging studies as well as suggesting new improvements of traditional models. The crucial observation is that in the tight-packing limit, $x \rightarrow 1$, the divergence of $f(x)$ is entirely controlled by the logarithmic term which is independent of both ϵ and h . This result provides a theoretical framework for explaining the numerical findings of Ref.⁶ who ascertained that the force loading curve was not too sensitive to the potential strength and sign at high packing densities. In other words, from this simple mean-field treatment we have an indication that a resistance to dense confinement comes from entropic effects rather than polymer self-interactions or flexibility. This is also in agreement with the picture proposed in Ref.¹².

To the best of our knowledge the fact that also the finite thickness of DNA is responsible for its elastic properties has not been fully investigated before, and hence is the focus of the present study. Usually, in beads-and-springs models, excluded volume effects are incorporated at the level of hard-core repulsion between pairs of coarse-grained beads. However, the most satisfactory way to account for steric effects is through the modelling of the polymer chain as a tube with finite uniform thickness, Δ , rather than a series of beads connected by one-dimensional springs. The appropriate treatment of the chain thickness usually leads to remarkably different physics than with traditional beads-and-springs models. A striking example is provided by the natural emergence of protein-like secondary motifs in marginally-compact conformations of thick chains¹⁵.

The finite thickness impacts on two distinct features of polymer conformations. On one hand it will constrain the local radius of curvature to be not less than Δ to avoid singularities. This effect induces naturally a bending rigidity on the polymer. As will be shown later, the resulting persistence length depends crucially on Δ , so that the latter appears to be a decisive factor for the huge difference of the persistence length for single-stranded and double stranded DNA, as we shall show later. On the other hand there is also a non-local effect due to the fact that any two portions of the tube, at a finite arclength separation, cannot interpenetrate. Equivalently, the centerlines of the two portions need to be at a distance greater than 2Δ (see Fig. 1).

In traditional beads-and-springs models it is only this second effect that is taken into account through pairwise hard-core repulsion. Interestingly, one needs to go beyond pairwise interactions to account for the above mentioned effects in discretised polymer chains. This is best illustrated considering the discrete succession of equispaced "beads", $(\vec{r}_1, \vec{r}_2, \dots, \vec{r}_N)$, as the centerline of a tube with thickness Δ . The requirement on the local radius of curvature is simply enforced by finding the radii of the circles going through any consecutive triplet of points and ensuring that each of them is greater than Δ . The non-local effect can be addressed within the same framework by considering the minimum radius among circles going through any non-consecutive triplet of points. This radius is precisely the distance of minimum approach and, again, has to be greater than Δ . In summary,

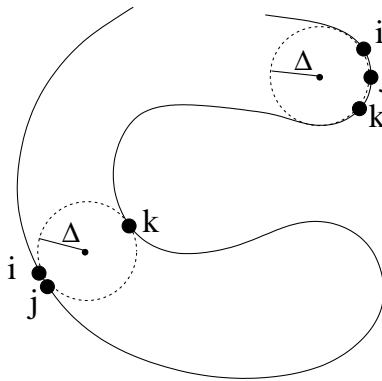


FIG. 1: In order for a curve to be a viable centerline for a tube of uniform thickness Δ it is necessary that the radii, r_{ijk} of the circles going through any triplet of points on the curve i, j, k are not smaller than Δ . This requirement forbids the presence of tight local bends incompatible with the tube thickness as well as unphysically proximity of distinct portions of the centerline.

the appropriate treatment for the finite thickness, Δ , of the tube associated to a discretized centerline is reflected in the fact that the radii of the circles going through any triplet of distinct points has to be greater than Δ ¹⁶.

One is thus naturally led to consider the following Hamiltonian for the unconstrained, non self-interacting, double-stranded DNA:

$$\mathcal{H}(\Gamma) = \sum_{ijk} V_3(r_{ijk}) \quad (3)$$

where V_3 is the three-body potential used to enforce the thickness Δ of the chain^{15,16,17,18,19,20} and Γ is the configuration of the ds DNA. The argument of V_3 is the radius of the circle going through the triplet of distinct points i, j, k and has the form

$$V_3(r) = \begin{cases} 0 & \text{if } r > \Delta, \\ +\infty & \text{otherwise.} \end{cases} \quad (4)$$

The tube ends were modelled as hemispheres by introducing two “phantom” beads essentially coinciding with the terminal beads of the tube.

Since our experimental reference case is the packaging of genome inside the $\phi 29$ capsid, we take Δ as the thickness appropriate for hydrated double-stranded DNA: 1.25 nm while the spacing between the beads of our discretized tube is naturally taken as the average base spacing: $a = 0.34$ nm.

As stated earlier our goal is to describe the equilibrium thermodynamics of a self-avoiding thick chain of N beads confined in a sphere of radius R . In particular, we aim at calculating the free energy $F_N(R)$, for which it is straightforward to calculate the work done to package it under conditions of no energy dissipation, and also the quantity:

$$\Delta G_N(R) = F_N(R) - F_N(\infty). \quad (5)$$

The force that is necessary to apply in order to feed additional chain beads inside the sphere can be calculated by differentiating $\Delta G_N(R)$ with respect to N :

$$f \propto \frac{\partial \Delta G_N(R)}{\partial N}. \quad (6)$$

In principle, the free energy, $F_N(R)$ could be obtained through a Monte Carlo simulation where the conformation space is restricted to only those structures that can be confined in a sphere of radius not larger than R . This is, however, impractical due to the fact that in situations of high density (small R) it will be very difficult to move through distinct compact structures while respecting the confining constraints.

A useful alternative is to work in the conjugated ensemble where, instead of keeping fixed the radius of the confining sphere, R , one applies a uniform “hydrostatic” pressure, P that compactifies the chain. In this situation, the Boltzmann weight of a configuration, Γ is given by:

$$e^{-(E+PV)/K_B T} \quad (7)$$

where the temperature T is taken as the room temperature, $T = 300\text{ K}$, E is the structure energy calculated via Eq. (3) and V is the volume of the spherical hull associated to Γ . To find the radius of the spherical hull enclosing Γ we first determine the maximum distance, \bar{r} from the centre of mass of any of the beads in Γ . Since these beads lie on the centerline of a tube of thickness Δ , the required radius is $R = \bar{r} + \Delta$. It should be noted that, in principle, the smallest confining sphere is not necessarily centred on the centre of mass of Γ . However, we have verified by an explicit numerical search of the location of the centre of the smallest sphere that this approximation is very good when dealing with structures with good overall compactness, which are the focus of this investigation. We stress that E can take only two values, 0, and ∞ for configurations that are respectively compatible or incompatible with the thickness requirement. This effectively restricts structure space to the ensemble of viable conformations of the thick tube.

By working at fixed temperature, one can sample the configuration space for various values of P by using a standard Metropolis criterion. From the distribution (histogram) of the various hull volumes encountered at various pressures one can use an ordinary multiple histogram technique²¹ to recover the density of states, $W(R)$ corresponding to the number of viable structures (i.e. compatible with the preassigned thickness Δ) and hull radius R .

The required free energy, $F(R)$ is then:

$$e^{-\beta F(R)} \propto \sum_{R' < R} W(R') \quad (8)$$

The reconstructed free energy, $F(R)$, is defined up to an additive constant, which reflects the fact that the density of states can be obtained only up to a multiplicative constant. This additive constant is immaterial for the calculation of the packaging work and force in a system with a given number of beads, though it has to be set appropriately in order to simplify the scaling analysis of $F_N(R)$ as a function of N at fixed β . For this reason we have taken the unconstrained situation, $R = \infty$, as the reference case associated with zero free energy: $F_N(R = \infty) = 0$ (see Eq. 5).

It is worth to point out that the force estimate in (3) is for a chain that is fully confined in the cube, i.e. we have not considered the case of a chain that is partially contained in the cube while the remainder constitutes an external tail. The latter case may be closer to the *in vivo* condition; however, the contribution of the floating tail to the free energy is expected to become less and less important compared to that of the confined portion as $x \rightarrow 1$ in Eqs. 1 and 2, which is the limit case of interest. In addition, in experiments where the packaging force is probed, the protruding tail is kept under considerable mechanical tension and therefore is expected not to make significant contribution to the system entropy.

III. RESULTS

One of the paradigm models fruitfully used to describe DNA chains is provided by the freely-rotating chain²². Within this scheme a DNA chain is described as a succession of equally-long bond vectors, \vec{t}_i , subject to the constraint that consecutive bonds must be at a given angle, α . This constraint directly impacts on the chain persistence length (which measures how correlations between two bond vectors decrease with their arclength separation).

For a given length of the bond vectors, the bonding angle α has to be set *a posteriori* so to reproduce e.g. the experimental persistence length, ξ . It is appealing to notice, as pointed out before, that the notion of intrinsic thickness of the DNA chain, naturally impacts on the minimum attainable radius of local curvature and hence on the allowed range of the bonding angle, α . This leads to the existence of a non-trivial persistence length, ξ , induced by the chain thickness. Such dependence can be estimated as follows. Consider a discrete chain of thickness Δ , with the consecutive unitary bond vectors $\vec{t}_i \equiv \vec{r}_{i+1} - \vec{r}_i$ and \vec{t}_{i+1} . The constraint over the bonding angle is give by

$$\vec{t}_i \cdot \vec{t}_{i+1} \geq 1 - \frac{1}{2\Delta^2}. \quad (9)$$

Neglecting the effects of the chain self-interactions it is possible to calculate explicitly the quantity $\langle \vec{t}_n \cdot \vec{t}_m \rangle$, with $n < m$, which defines in turn a persistence length, ξ via $\vec{t}_n \cdot \vec{t}_m \sim \exp\left(-\frac{|n-m|}{\xi}\right)$. One thus obtains that $\xi(\Delta)$ is given by

$$\xi(\Delta) = -\frac{1}{\log(1 - (2\Delta)^{-2})}. \quad (10)$$

This approximate relationship can be specialized to the case of double-stranded DNA, where the unit bonds are taken as the base spacing, 0.34 nm and the thickness equal to the radius of hydrated dsDNA, 1.25 nm. One thus observes $\xi = 19\text{ nm}$, which is about one half of the correct experimental value $\xi_{exp} \approx 50\text{ nm}$. This theoretical estimate, which takes into account the mere effect of steric hindrance of the chain does not include the contribution of electrostatic repulsion of the phosphate groups to the apparent persistence length²³ but appears to capture the correct order of magnitude of the observed persistence length.

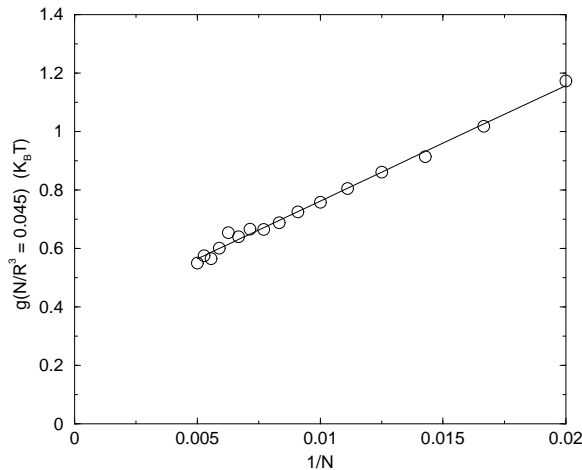


FIG. 2: Curves for the reduced free energy at the fixed density $N/R^3 = 0.045$ for values of N in the range $50 \leq N \leq 200$.

As a further validation of this approach it is worth considering the case of single-stranded DNA. In this case the vector length is equal to ~ 5 Å, which is the typical nucleotide separation projected on a line interpolating the chain, while the thickness is about ~ 4 Å. The near equality of these two parameters imply that the thickness induced persistence length of single-stranded DNA is comparable with the nucleotide spacing, and in fact one obtains, $\xi \sim 1$ nm. Again, this is consistent with the experimental data for ssDNA in solutions of high ionic strength (which screen the phosphate charges) for which values for ξ of the order of 1 nm are observed²⁴.

Given the simplified derivation of the parametric dependence of ξ on Δ and the total absence of adjustable parameters in the theory, this agreement is remarkable and testifies the need to model explicitly the DNA intrinsic diameter.

While the soluble models leading to e.g. the results of eqns (3) and (10) are useful for gaining insight in the basic physics of thick polymers, they cannot be used to fully characterize more complicated instances such as the packaging process. To address this issue it is, therefore, necessary to resort to stochastic numerical simulations. In the present study, the equilibrium properties of the thick polymer was characterised by a multiple Markov chain simulation²⁵ where several copies of the system each at a different pressure were evolved simultaneously. The evolution was controlled by the Metropolis acceptance of elementary chain distortion involving crankshaft, pivot and slithering moves²⁶. A preliminary measure of correlation times allowed to collect statistically independent measures for reconstructing the density of states as described in the methods section. The full equilibrium thermodynamics was thus obtained for tubes with a discrete number of beads, N . Values of N up to 200 were considered here. As was argued before, in the limit of large N the free energy should be extensive in N at fixed filling fraction, N/R^3 . Therefore we expect $F_N(R)$ to obey the following scaling relations:

$$\lim_{N \rightarrow \infty} F_N(R) \sim N g \left(\frac{N}{R^3} \right), \quad (11)$$

which enables, for large N , to express the confining force as a function of g :

$$a f_N(R) = \frac{\partial F}{\partial N} \sim g \left(\frac{N}{R^3} \right) + \frac{N}{R^3} g' \left(x \right) \Big|_{x=N/R^3}. \quad (12)$$

where $a = 0.34$ nm is the unit length in our model. Note that the same scaling theory applies also to expressions (1) and (3). These relations will be obeyed only approximately for any finite chain, though such corrections decay for increasing values of N , as shown in the following.

In Fig. 3 we have plotted the reduced free energy, $g_N = F_N(R)/N$ as a function of N/R^3 for different values of N . It is apparent that, as the size of the system, N , increases, the curves for g_N deviate less from each other, indicating the decrease of finite-size corrections from the limit curve of expression (11). Indeed, the systematic decay of such corrections for increasing N is visible in Fig. 2 where we have reported the trend of g_N as a function of N^{-1} at a fixed density. As visible in Fig. 3, the data are well interpolated by a linear regression with correlation coefficient $r \sim 0.98$. Through such regression one can estimate the error on the extrapolated value for g as the error on the intercept. The observed correlation coefficient is statistically significant, since it pertains to 16 data points and is suggestive that finite-size corrections decay approximately as N^{-1} . However, from the systematic decrease of the linear regression slope observed when fitting data for the larger tube lengths only, it can be argued that the convergence is faster than $1/N$ and may also be compatible with decays such as $N^{-1.5}$.

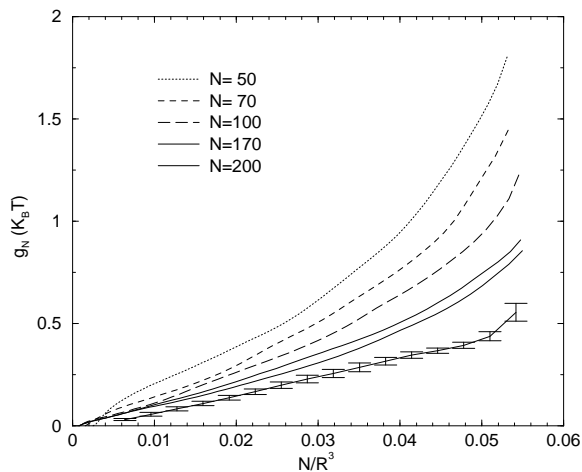


FIG. 3: The reduced free energy as a function of the packing density, N/R^3 for the indicated values of N . The bottom curve is obtained by extrapolating the finite-size curves for $N \rightarrow \infty$.

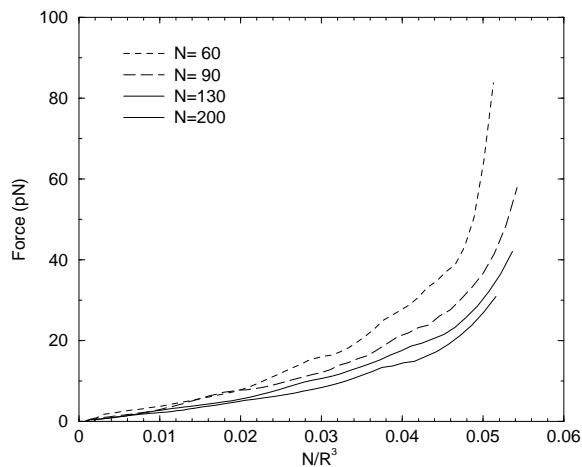


FIG. 4: Curves for the force necessary to apply to package the thick tube to the required density, N/R^3 . The curves for the force are obtained from simulations with the indicated number of beads, N .

The same rate of convergence of finite-size corrections is inherited by the force obtained from (12) by using g_N instead of g . By considering several values of N one obtains a succession of curves for the loading force that, again, appear to approach a limiting curve from above. This is in agreement with the physical intuition that more force is required to pack a shorter (but equally thick) chain to the same target density.

As for the corrections to g , also the force curves appear to approach the limit curve of interest at a rate somewhat faster than $1/N$. Nevertheless, since we cannot give a precise account of the correction exponent we calculated the limit force by using the conservative $1/N$ decay estimate and by fitting only the data of the largest tube lengths, $100 < N \leq 200$. The results are provided in Fig. 5 and can be compared with the experimental curve of ref.⁴ as discussed below.

If one considers the prolate $\phi 29$ capsid as an ellipsoid the reference density at full genome packaging as $x = 0.063$. The largest densities reached in our simulation correspond therefore to about 85 % of this value. Neglecting the contribution of the protruding tail in the $\phi 29$ experiment one can then compare the experimental force at 85 % genome packaging, 34 pN, with our peak force of 16 pN, which appear to be correct within only a factor of two. We stress that this finding exploits only the severe restrictions in configuration space operated by the finite thickness of DNA itself; it is striking that this entropic effect appears to account for half the force observed in the experiment. Furthermore, the limit curve for the force has been obtained with the conservative $1/N$ estimate of the decay of finite-size corrections; this arguably leads to an underestimation of the force required to package the DNA chain.

Another quantitative comparison against the experiment can be done considering the total packaging work. The experimental total packaging work in the experiment of ref.⁴ was estimated as $2 \cdot 10^4 K_B T$, corresponding to $1.04 K_B T$ per base pair (or

bead in our model). In our case, the work per bead necessary to package the tube to a preassigned density, x , (starting from an unconstrained situation) is given simply by $g(x)$ (see Fig. 2). As before, we can connect the peak density reached in our simulation with the experimental situation where 85 % genome is packaged in the capsid. The value of g observed in our model at this density corresponds to $0.55 K_B T$, which differs by less than a factor of two from the experimental work (but the latter refers to 100 % packaging). In summary, even without accounting for the different final densities in the experiment and in our model, we can nevertheless conclude that also a substantial fraction (more than 50%) of the work required to package DNA could result from the entropic cost of compactifying a polymer of finite thickness. These results are also consistent, *a posteriori*, with the findings of Ref.⁶, where it was pointed out that the detailed form (and even sign) of the DNA self-interaction was not the determinant factor in the packaging process. The important role played by the loss of configurational entropy in DNA packaging or condensation is also supported by recent numerical and analytical work^{27,28}.

As we argued before, the finite DNA thickness appears to account for a significant fraction of the physical properties (such as persistence length and resistance to confinement) that are usually ascribed entirely to DNA self-interaction and bending rigidity. As an extension of the model discussed so far, one is lead to consider the case where, on top of the finite-thickness treatment one adds bending rigidity effects. The latter are customarily taken into account by the following energy term:

$$E_{b.r.} = \frac{K_B T}{2} \xi \int ds \frac{1}{R(s)^2} \quad (13)$$

where the integral runs over the DNA contour, R denotes the local curvature and ξ is the persistence length. In a model which already incorporates DNA thickness the use of the full persistence length in expression (13) certainly overemphasizes the elastic effects (since thickness alone can satisfactorily account for a significant fraction of the DNA persistence length, ξ). Even in this situation it will be apparent that the additional (overestimated) force increment ascribable to the presence of bending rigidity is of the same order of the one induced by the thickness.

As a first step we provide an upper bound for the confining force increment of the due to the added elastic term. To this purpose let us consider a thick chain that has been compactified so to nearly fill a given cavity. It is assumed that packing conditions are such that there is almost no structural freedom left for how to add an additional bead inside the hull. In particular, the bead has to be added so to achieve the tightest local curvature of the chain. Since the lower bound for the curvature is the thickness itself, Δ , the additional packaging force is estimated as:

$$\Delta f_{b.r.} = \frac{K_B T \xi}{2\Delta^2}. \quad (14)$$

Using $\xi = 50nm$ as in Ref.⁶ and $T = 300 K$ one obtains that an upper bound for the force increment due to bending rigidity is $\Delta f_{b.r.} \approx 66$ pN. To obtain a more accurate estimate of Δf we have undertaken additional studies where the numerical scheme previously discussed for the confined thick chain was generalised to include explicitly the bending rigidity term of eq. (13).

The augmented difficulty of packaging the chain in this situation resulted in the fact that the maximum density achieved was $N/R^3 = 0.050$, corresponding to 80 % of the estimated packing fraction of ϕ_{29} . In this case, the confining force for a chain of

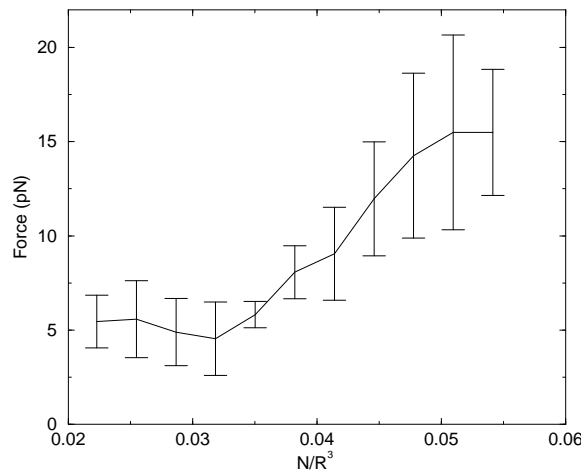


FIG. 5: Plot of the extrapolated force required to package an infinitely long tube to the preassigned density, N/R^3 . The force is expressed in picoNewtons. The estimated packing density of the fully-loaded ϕ_{29} capsid corresponds to 0.063 .

200 beads resulted equal to 39 pN. This corresponds to an extra force of around 12 pN, (the pure thickness-induced force at the same filling fraction is ~ 27 pN, see Fig. 4). This value overestimates the bending rigidity contribution in the thermodynamic limit due to the systematic decrease of the force as a function of chain length. However, even allowing for the overemphasized contribution of bending rigidity due to both finite-size effects and the use of the full persistence length ξ in eq. (13) one can already conclude that the finite-thickness effects are comparable with those associated with bending rigidity (see. Figs. 4 and 5).

This conclusion remains true when finite-size extrapolation is carried out on this second model using chains of 40, 80, 100, 120, 160 and 200 beads. From the thermodynamic data a total force of 24 ± 7 pN can be extrapolated at the highest densities $N/R^3 = 0.050$. Despite the still simplistic nature of the second model considered here, the extrapolated force appears to be fully consistent with the experimental results for $\phi 29$ at the corresponding filling fraction of 80 %, where a total force of 27 pN was recorded. Thus, the different calculations presented here all indicate that the contribution to the resistance to packaging arising from the finite DNA thickness is comparable to that of other terms usually considered in coarse-grained models of DNA. This indicates that various phenomenological properties of DNA can be accounted in a more accurate and complete way by including an explicit modelling of DNA thickness besides the traditional terms in the effective Hamiltonian.

Finally, it is interesting that, consistently with the study of ref.⁶ and with other theoretical studies^{7,27} the most compact conformations obtained in our stochastic simulations (in thermodynamic equilibrium) show the marked tendency to occupy the spherical cavity by performing a succession of turns in a spool-like fashion with a portion of the tube, while the remainder of the chain fills the space around the spool axis, as visible in Fig. 6.

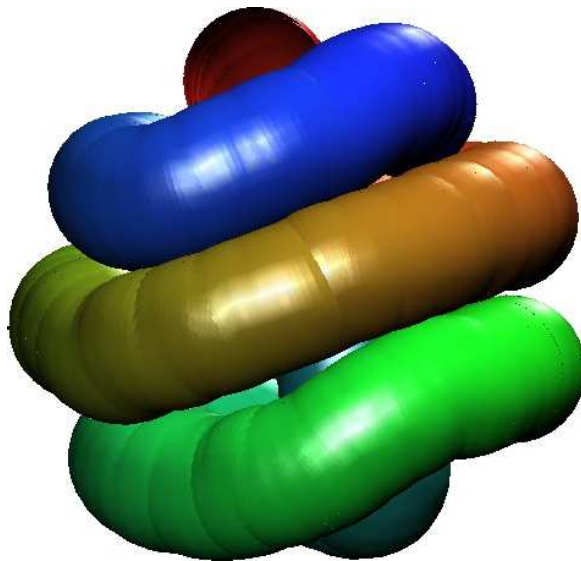


FIG. 6: Example of a highly compressed conformation for a discrete tube of 200 beads and thickness $\Delta = 3.7$ (in units of the bead spacing).

IV. CONCLUSIONS

We have characterized the equilibrium thermodynamics of a polymer chain with finite thickness confined inside a spherical cavity. The model aims at schematizing the packaging of the genome (double-stranded DNA) inside a bacteriophage capsid. Stochastic simulations and reweighting techniques were used to calculate the force (and work) required to compactify to a given density a discrete tube of up to 200 beads. The sole inputs of the model are the experimental values for the spacing of the base pairs in double-stranded DNA, and the thickness of the latter; no tunable parameters or specific forms of self-interaction of the polymer are introduced. By using finite-size scaling techniques we have estimated the force necessary to package the genome inside the $\phi 29$ virus. The predicted force (and packaging work) agrees with the experimental one to within a factor of two, thus testifying the importance of an appropriate modelling of the DNA thickness in the packaging process. This fact is further corroborated by a theoretical calculation which shows that the different thickness of single- and double-stranded DNA can satisfactorily account for the large difference of the respective persistence lengths.

ACKNOWLEDGMENTS We are grateful to S. C. Harvey, T. Odijk and A. Maritan, for illuminating discussions and sugges-

tions. We acknowledge financial support from INFM and Murst Cofin 2001.

-
- ¹ Grimes, S., Jardine, P. J. & Anderson, D. (2002). Bacteriophage phi 29 dna packaging. *Adv. Vir. Res.* **58**, 255–294.
 - ² Riemer, S. C. & Bloomfield, V. A. (1978). Packing of dna in bacteriophage heads: some considerations on energetics. *Biololymers*, **17**, 785–794.
 - ³ Homa, F. L. & Brown, J. C. (1997). Capsid assembly and dna packaging in herpes simplex virus. *Rev. Med. Virol.* **7**, 107–122.
 - ⁴ Smith, D. E., Tans, S. J., Smith, S. B., Grimes, S., Anderson, D. L. & Bustamante, C. (2001). The bacteriophage phi29 portal motor can package dna against a large internal force. *Nature*, **413**, 748–752.
 - ⁵ Simpson, A. A. & coworkers (2000). Structure of the bacteriophage phi 29 dna packaging motor. *Nature*, **408**, 745–750.
 - ⁶ Kindt, J., Tzllil, S., Ben-Shaul, A. & Gelbart, W. M. (2001). Dna packaging and ejection forces in bacteriophages. *Proc. Natl. Acad. Sci. USA*, **98**, 13671–13674.
 - ⁷ Odijk, T. (1998). Hexagonally packed dna within bacteriophage t7 stabilized by curvature stress. *Biophysical Journal*, **75**, 1223–1227.
 - ⁸ Pais, A. A. C. C., Miguel, M. G., Linse, P. & Lindman, B. (2002). Polyelectrolytes confined to spherical cavities. *J. Chem. Phys.* **117**, 1385–1394.
 - ⁹ Muthukumar, M. (2001). Translocation of a confined polymer through a hole. *Phys. Rev. Lett.* **86**, 3188–3191.
 - ¹⁰ Hansen, P. L., Podgornik, R. & Parsegian, V. A. (2001). Osmotic properties of dna: critical evaluation of counterion condensation theory. *Phys. Rev. E*, **64**, 021907.
 - ¹¹ Cerritelli, M. E., Cheng, N. Q., Rosenberg, A. H., McPherson, C. E., Booy, F. P. & Steven, A. C. (1997). Encapsidated conformation of bacteriophage t7 dna. *Cell*, **91**, 271–280.
 - ¹² Strey, H. H., Podgornik, R., Rau, D. C. & Parsegian, V. A. (1998). Dna-dna interactions. *Curr. Opin. Struc. Biol.* **8**, 309–313.
 - ¹³ Doniach, S., Garel, T. & Orland, H. (1996). Phase diagram of a semiflexible polymer chain in a theta solvent: application to protein folding. *J. Chem. Phys.* **105**, 1601.
 - ¹⁴ Lise, S., Maritan, A. & Pelizzola, A. (1998). Bethe approximation. *Phys. Rev. E*, **58**, R5241.
 - ¹⁵ Maritan, A., Micheletti, C., Trovato, A. & Banavar, J. R. (2000). Optimal shapes of compact strings. *Nature*, **406**, 287.
 - ¹⁶ Gonzales, O. & Maddocks, J. H. (1999). Global curvature, thickness and the ideal shapes of knots. *Proc. Natl. Acad. Sci. USA*, **96**, 4769–4773.
 - ¹⁷ Katrich, V., Olson, W. K., Pieranski, P., Dubochet, J. & Stasiak, A. (1997). Properties of ideal composite knots. *Nature*, **388**, 148–151.
 - ¹⁸ Banavar, J. R., Gonzales, O., Maddocks, J. H. & Maritan, A. (2003). Self intersection of strands and sheets. *J. Stat. Phys.* **110**, 35–50.
 - ¹⁹ Stasiak, A. & Maddocks, J. H. (2000). Best packing in proteins and dna. *Nature*, **406**, 251–253.
 - ²⁰ Banavar, J., Maritan, A., Micheletti, C. & Trovato, A. (2002). Geometry and physics of proteins. *Proteins: Structure Function and Genetics*, **47**, 315–322.
 - ²¹ Ferrenberg, A. M. & Swendsen, R. H. (1989). Optimized monte-carlo data-analysis. *Phys. Rev. Lett.* **63**, 1195–1198.
 - ²² Flory, P. (1989). *Statistical mechanics of chain molecules*. Hanser Publisher, Munich.
 - ²³ Rybenkov, V. V., Cozzarelli, N. R. & Vologodskii, A. V. S. (1993). Probability of dna knotting and the effective diameter of the double helix. *Proc. Natl. Acad. Sci. USA*, **90**, 5307.
 - ²⁴ B. Tinland, A. Pluen, J. S. & Weill, G. (1997). Persistence length of single-stranded dna. *Macromolecules*, **30**, 5763–5765.
 - ²⁵ Tesi, M., van Rensburg, E. J., Orlandini, E. & Whittington, S. (1996). Monte-carlo study of the interacting self-avoiding walk in t three dimension. *J. Stat. Phys.* **82**, 155–181.
 - ²⁶ Sokal, A. D. (1997). Dna packaging and ejection forces in bacteriophages. *Nuclear Physics B*, **Suppl. 47**, 172–179.
 - ²⁷ Arsuaga, J., Tan, R. K. Z., Vazquez, M., Sumners, D. W. & Harvey, S. C. (2002). Monte Carlo methods for the self-avoiding walk *Biophys. Chem.* **101**, 475–484.
 - ²⁸ Odijk, T. (1993). Physics of tightly curved semiflexible polymer-chains. *Macromolecules* **26**, 6897–6902.